Available online at www.jourcc.com

Journal homepage: www.JOURCC.com

Journal of Composites and Compounds

Mechanical and electrochemical behaviors assessments of Aluminum-Graphene Oxide composites fabricated by mechanical milling and repetitive upsetting extrusion

Amirhossien Bahri [a], Reza Askarnia [a], Javad Esmaeilzadeh [b], Sajede Roueini Fardi [c]*

[a] Faculty of Materials and Metallurgical Engineering, Semnan University, Semnan, Iran
[b] Faculty of Materials and Chemical Engineering, Esfarayen University of Technology, Esfarayen, North Khorasan, Iran
[c] Faculty of Materials Science and Engineering, K.N. Toosi University of Technology, Tehran, Iran

ABSTRACT

This study is aimed to fabricate the Aluminium-graphene oxide (Al-GO) composites with different concentration of GO (0.5, 1, and 2 wt. %) at 300 °C using repetitive upsetting extrusion (RUE) technique. Uniform dispersion of GO nanoplates throughout the matrix was obtained by sequence processes including the ultrasonicating, ball milling and RUE. The microstructure of composites was investigated by X-ray diffraction, scanning electron microscope and Raman analysis. The results confirmed that the Al-1GO illustrated the uniform and homogenous dispersion of GO into the Al matrix. Raman results confirm the absence of aluminum carbide phase formation during the RUE process. The mechanical properties results show the greater hardness, compressive strength and yield strength of Al-1GO than other ones. This 500% enhancement of Al-1GO in mechanical behavior may be related to desired dispersion of GO throughout the matrix. Current density of the Al matrix corrosion significantly increased from 2.65 to 15.21 (μA/cm^2), when the amount of GO increased from 0 to 2 wt. % due to galvanic corrosion at the presence of the GO reinforcement.
Peer review under responsibility of JCC Research Group

ARTICLE INFORMATION

Article history:
Received 9 July 2021
Received in revised form 18 August 2021
Accepted 23 September 2021

Keywords:
Al matrix
Graphene oxide
Composites
Mechanical properties
Hardness
Repetitive upsetting extrusion

1. Introduction

Aluminum matrix composites are used in several industries (automotive, aerospace and military) due to low density, good weight strength, thermal and electrical conductivity [1]. Researchers used various reinforcement (Al_2O_3, B_4C, CNT) to improve the mechanical properties of aluminum matrix [2–4]. Among all the reinforcement, graphene oxide (GO) has attracted a lot of attention due to its excellent mechanical properties, electrical properties and low density [5–7]. For metal and metal matrix composites, sever plastic deformation (SPD) can introduce large plastic strains and lead to creation of fine grains, which can consequently improve the mechanical properties [8]. Fine-graining can be done by many techniques such as high-pressure torsion (HPT) [9], accumulative roll bonding (ARB) [10], and angular equal channel pressure (ECAP) [11], twist extrusion (TE) [11], as the most common ones. These techniques are usually applied in cyclic fashion, meaning that a high amount of tension (and strain) is stored in the materials over many cycles, without substantially changing the sample size and shape [12]. For example, Huang et al. [12] prepared aluminum/graphene composites by HPT and reported improvement in the stiffness and tensile strength compared to pure Al. Hot ARB technique was also tested for preparation of Al-graphene composites and ~73% improvement (5 wt. %) in mechanical properties, relative to pure Al, was obtained [13]. Another technique that was applied is ECAP with considerable increase in strength and hardness with 0.25 wt. % graphene addition. The main advantage of the SPD techniques is that the strength of the materials can be increased without requirement of any additional thermal heat-treatment [14]. This is particularly important for metal-graphitic materials composites (e.g., Al-Graphene), since heat treatment can lead to formation of brittle phases (e.g., Al_4C_3), which can potentially deteriorate the mechanical properties of the composites [15, 16]. In contrast to these techniques, repetitive upsetting-extrusion (RUE), as another SPD method, has been demonstrated recently as a promising technique for enhancing the mechanical properties of metallic alloys and composites [17]. RUE is basically a hybrid process of simultaneous exertion of continuous pressure and extrusion in a cyclic fashion, having the potential to yield high number of strains uniformly distributed in the materials [18]. This leads to a fine, but homogeneous grain size distribution in the materials matrix, and consequently to an increased yield strength [18]. Additionally, among all SPD techniques, RUE along with HPT can results in highest amount of strain during the cycle in the materials matrix. Higher amount of strain can potentially result in more homogeneous reinforcement distribution in the composite matrix [19]. This is particularly critical in metal-graphitic materials composites, since there is considerable tendency in the graphitic materials to agglomerate, which usually is accompanied with

* Corresponding author: Reza Askarnia; E-mail: rezaaskarnia96@semnan.ac.ir
DOR: 20.1001.1.26765837.2021.3.8.1.8
https://doi.org/10.52547/jcc.3.3.1

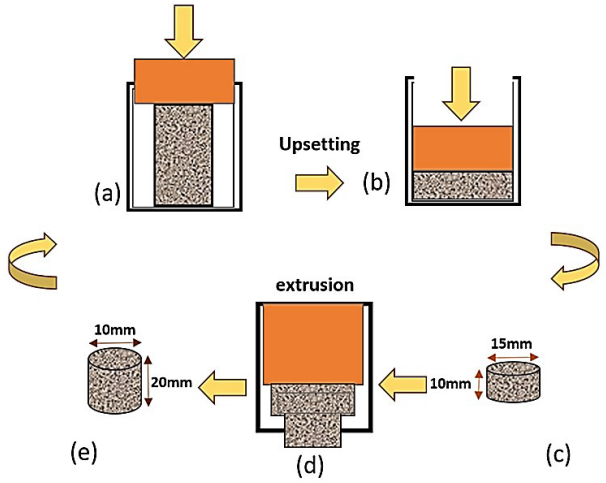

Fig. 1. Schematics of forming process including consecutive processes of hot pressing and extrusion.

degradation in the composite final properties [20, 21]. Binesh et al. [22] applied RUE process to Al7075 alloy at 250 °C with different number of passes (1 to 4 passes) and observed significant mechanical properties (yield and final stress) improvement as the pass number increased. In another work, Gao et. al evaluated the microstructural evolution of Al-Li alloy with application of up to 3 passes at 350 °C, and reported vanishment of dislocations due to recrystallization. Presumably, the removal of dislocations is related to the application of escalated temperature (350 °C), which allows extensive atomic rearrangement and consequent elimination of dislocations through formation of sub-grain boundaries. In spite of the potentials of the RUE technique, it has not yet been exploited for the preparation of Al/graphitic materials (e.g., graphene, graphene oxide, carbon nanotube) composites.

To the best of the authors' knowledge, there isn't a report on the fabrication of Al-GO composite via RUE process. We used RUE technique (with fixed optimized pass number) at 300 °C and fabricated Al-graphene oxide composite with varying concentration of graphene oxide (0, 0.5, 1, 2). We also evaluated the hardness and compressive strength of the composites. The results show that the Al-GO composite produced by the RUE process possesses desirable mechanical properties that are comparable with those results reported for Al-GO composites produced by other techniques.

2. Experimental Procedure

2.1. Material and methods

In the first stage, Graphene sheets used in our experiments were prepared by modified hummers method as reported previously [23]. The mixture of Al (average particle size of 40 µm, 99.5 wt. % pure, Merck, Germany) and GO were prepared in wet state. GO was ultrasonicated for 30 min in ethanol medium in order to deagglomerate the GO powder. Afterward the aluminum powder was slowly added to the GO suspension being stirred for 6 h rigorously by a magnetic stirrer (stirring speed: 600 rpm). Then, the mixture ball milled in a stainless-steel jar with ball to powder ratio of 5 to 1 at 200 rpm for 4 h. The size of the Al powders decreased at initial of ball milling, and thereafter, they were cold-welded and their size increased. However, GO can operate as a barrier against cold-welding and, consequently, the increasing GO decreases the powder size. As the last step of powder preparation, the suspension underwent drying for 24 h at 65 °C, to get rid of ethanol. In the current work three types of powders were prepared with different content of GO (0.5, 1 and 2 wt. %). After the powder preparation, as Figure. 1 show, the powders were formed using RUE technique exploiting two stages of pressing and extrusion. During the former, the sample length decreases substantially and accordingly its cross-sectional area increases, while during the latter process, the length of the sample increases and its cross-sectional area decreases. For this reason, powders were initially pressed at 300 °C using a single-axis hydraulic press with jaw movement speed of 50 mm/min. The pressing die was made of graphite and its diameter and length were 15 mm and 10 mm, respectively. As the pressing stage was over, the sample look liked a short cylinder. Then, the formed cylinder underwent an extrusion process at 300 °C in a similar die made of graphite with diameter and length of 10 mm and 20 mm, respectively. The force applied for extrusion was 1 ton during 10 min. The samples were then cooled in water immediately after the extrusion process. The process was repeated for three times (three passes) for each sample in order to obtain a considerable amount of uniform distribution of strain.

2.2. Characterizations

The formed cylinders were polished using SiC grinding papers (up to 4000 grit), and then the contained phases were characterized by Bruker D8 Advance diffractometer (Billerica, MA, America) operating in the reflection mode with Cu-Kα radiation (35 kV, 30 mA) and diffracted beam monochromator, using a step scan mode with the step size of 0.05° (2θ) and scan range of 10-90° (2θ). Raman spectroscopy (model: RMP-335, Japan) was measured with a wavelength of 633 nm to investigate disorder in the graphene oxide structure. Fourier-transform infrared spectroscopy (FT-IR, Spectrum RX I, PerkinElmer, Waltham, Massachusetts, New England, USA) was applied to investigate the chemical bonding in the wavelength range of 400–4000 cm^{-1}. The microstructural features (porosities, cracks, agglomeration and distribution of GO, grain refinement) of the samples were analyzed using scanning electron microscopy (FE-SEM, MIRA3, TESCAN, Brno–Kohoutovice, South Moravian Region, Czech Republic)) equipped with energy dispersive spectrometer operating at 15 kV. Vickers hardness measurement was conducted

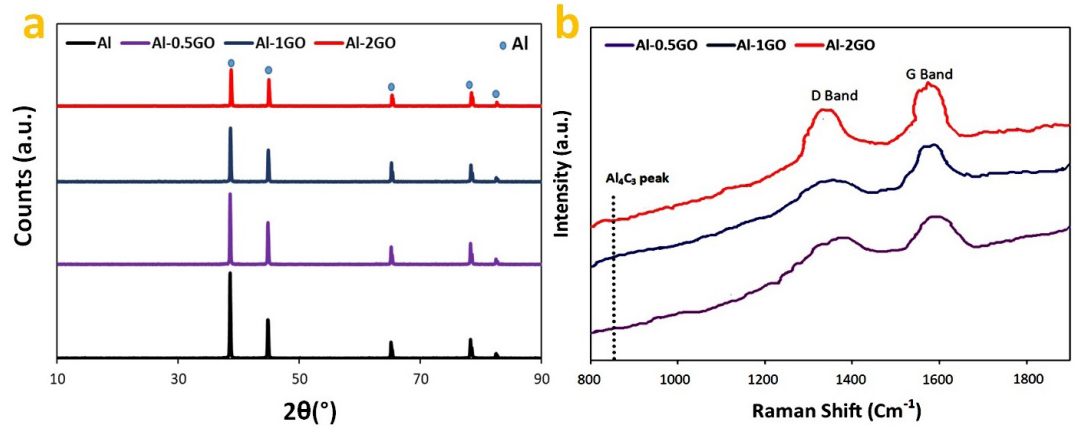

Fig. 2. (a) XRD patterns (b) Raman spectroscopy of Al-GO nanocomposites.

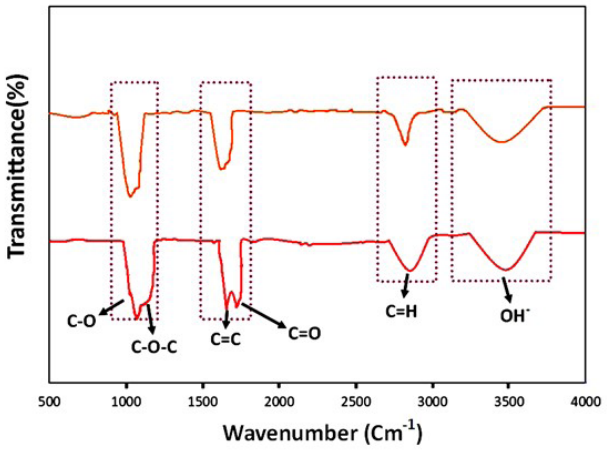

Fig. 3. FT-IR of Al-1GO nanocomposite after RUE process.

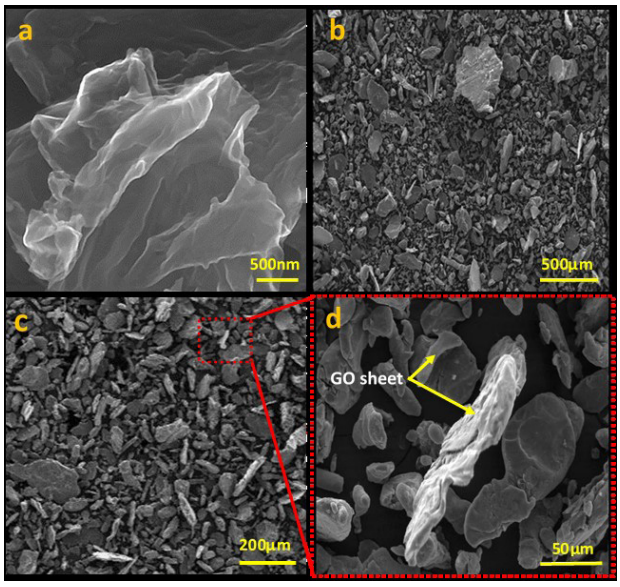

Fig. 4. SEM images of (a) GO nanosheet (b) Al pure (c, d) different magnification of Al-2GO powder.

using a digital micro hardness tester (HVS-1000, Oceanus, Xuanwu District, Beijing, chin) under 500 g load for 15 seconds. The density of samples was measured by the Archimedes technique. The compressive strength was carried using a universal test machine (STM-400 Cap. 400 kN, SANTAM Engineering Design Co. Ltd., Tehran, Iran) at a constant compression rate under standard ASTM E9-09. The potentiodynamic polarization experiment was conducted in 3.5 wt. % NaCl solution, at a scan rate of 1 mV/s and potential range of −0.25 V to +0.25 V.

3. Result and Discussion

3.1. morphology and microstructure analysis

Figure 2(a) shows the XRD results of the aluminum/GO composites after three passes of RUE process. As seen, aluminum peaks of (111), (200), (220) and (311) planes are observable at 38.6°, 44.85°, and 65.2°, 78.3° angles, respectively. As expected, no peaks related to GO (2θ ≈11°) was observed in any samples which could be due to its low contents in composites [23]. It was reported that GO could react with Al and produce Al_4C_3 or Al_2O_3 phases during high temperatures process of composites manufacturing [24, 25]. The formation of these phases throughout the composites can be detrimental for composites mechanical properties, due to their brittle features. These phases could also act as nucleation sites in the composite matrix, potentially leading to microcracks formation and consequent decrease of the composite strength. According to XRD pattern of these samples, neither Al_4C_3 nor Al_2O_3 is formed in the composites, which is believed to be due to the applying of low temperature RUE process (300 °C).

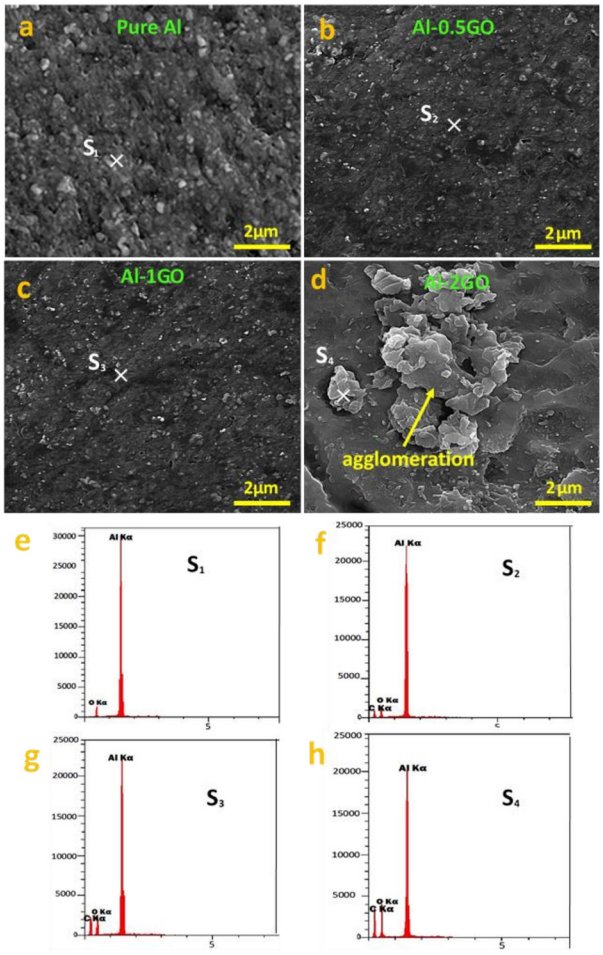

Fig. 5. (a-d) SEM images of Pure Al and it's nanocomposites. (e-h) EDS spectra of yellow rectangle in corresponding nanocomposite.

The Raman spectrum of graphene-based materials possesses the two major bands of D and G between 1200-1800 cm^{-1} wave number (Figure 2(b)). The D band at 1360 cm^{-1} determines the presence of defects as well as disorders in GO structures resulted of impurities [26]. The G band at 1580 cm^{-1} region is also attributed to common C-C bonds which is observable at all graphite-based materials. The intensities of disordering and defects content in GO show in table 1 by calculating the bands intensity ratio of ID/IG. The increasing of GO contents in composites decrease the ID/IG ratio due to high volume impacts between balls and GO nanoparticles during ball mills. Hence, the lower ID/IG of Al-1GO in comparison with other composites determine the lower amounts of disorders and defects in GO and preserving of GO structure [27]. Besides, the Raman results illustrate no chemical reactions between Al and GO, so, there is no peak at 850 cm^{1-} attributed to Al_4C_3 brittle phase [28,

Table 1.
Extracted data from Raman spectroscopy

Sample	Al-0.5GO	Al-1GO	Al-2GO
RS GO	1594	1592	1589
ID/IG	0.88	0.84	0.91

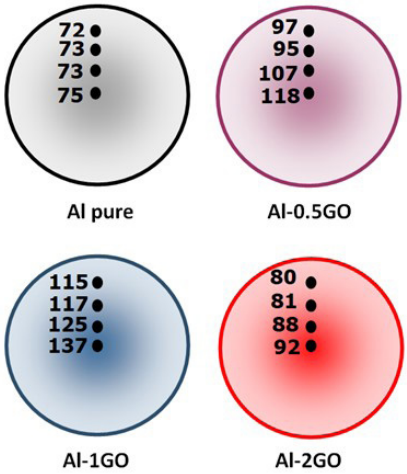

Fig. 6. Microhardness (HV) from the center to the edge of samples with different GO Content.

29]. It can be concluded that the RUE is an effective technique in order to fabricate Al-GO composites with no adverse chemical reactions. Since, the addition of other elements into GO nanoplates can decrease the temperature conversion of GO to reduced GO from 2000 down to around 500 °C [30], the FTIR analysis from Al-1GO powders and bulk specimens was taken to investigate the probable conversion of GO to reduced GO(RGO) (Figure 3). The peaks at 1634, 1108 and 2738 cm^{-1} are related to C-O, C=C and C-H bonds in stretching vibration modes, respectively [31]. The main peak at 3500 cm^{-1} shows the Hydroxyl groups in GO nanoplates [32]. Since, the major bond during the conversion of GO to RGO is revealed at 1750 cm^{-1}. Also, by conversion of GO to RGO, the C=O bonds are removed [33]. This is while, as can be seen in Figure 3, this bond is valid in both powders and bulks specimen's spectrums. It can be therefore found the RUE prevents to GO convert to RGO owing to lower processing temperature.

The Figure 4(a, b) reveals the morphologies of GO nanoplates, pure Al. The Figure 4(c, d) indicates that the ball milling process has been very effective in terms of making close contacts between Al particles and GO nanoplatelets. The well surrounding of the GO nanoplates with Al matrix has been presented by white arrows.

Figure 5 shows microstructure of pure Al, Al-0.5GO, Al-1GO and Al-2GO composite after RUE process. Homogeneous dispersion of graphene oxide plates is one of the major challenges in the formation of Al-GO composite. As can be also seen in figure 4, the matrix possesses the great uniformity in microstructure as well as fine grains which could be related to using of ball-mill process for composite powders preparation before RUE which can help to inhibit from GO nanoplates agglomerations. Also, the weak bonding between GO nanoplates will be broken through the RUE compression forces. As seen in Figure 5(b, c), the GO nanoplates in 0.5 and 1 wt. % amounts well uniformly dispersed throughout the matrix. While the increase in GO content up to 2 wt. % leading to form considerable agglomerates and reveal the heterogeneous distribution of GO into matrix (Figure 5(d)). These findings are due to inconsistency of bonding in GO and Al which composed of covalent and metallic bonds, respectively [34]. This covalent-metallic interface has a high interfacial energy, and as a result, GO nanoplates tend to form agglomerates throughout the metal matrix [35]. For this reason, in previous reported works [23, 35] applied no more than 2 wt. % of GO in order to avoid agglomeration formation and improve the mechanical properties of matrix. The Figure 5(e-h) the EDS spectra of the yellow rectangle in the corresponding samples. The EDS line scan profiles reveal the rare increase in amounts of O which may be related to the limited oxidation during ball mill process. Nonetheless, the XRD pattern reveals no Al_2O_3 peak.

Table 2.
Theoretical and experimental densities of pure Al and Al-GO nanocomposite

Sample	Pure Al	Al-0.5GO	Al-1GO	Al-2GO
Theoretical	2.70	2.698	2.694	2.690
Experimental	2.698	2.691	2.693	2.684

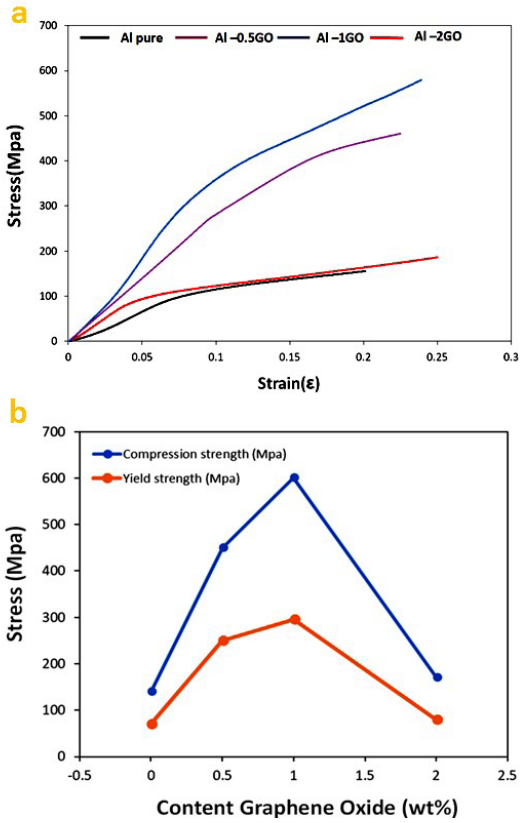

Fig. 7. (a-b) compressive strength-strain curves, calculated CS and YS of different samples, respectively.

3.2. Density and mechanical properties

The density of composites was measured using Archimedes' method. The all-measured densities of composites were listed in table 2 where the addition of incremental GO results in decrease of the composites densities. The similar results were observed in previous researches [23, 36]. It is obvious that the addition of GO with lower density (2.21 g/cm^3) than Al (2.7 g/cm^3) in composites lead to decline the composites densities. It should be noted that the deference between theoretical and practical densities are related to presence of porosities throughout the specimens.

Figure 6 presents the obtained hardness results of top and down surfaces of pure Al and its composites. As can be found, by increasing in GO content to 1 wt. % results in a 293% increase in micro hardness of composites. The obtained results also illustrate that the additions of 0.5 (118 HV) and 2 wt. % GO (92 HV) lead to lower increment of hardness compared to composites contain of 1 wt. % (137 HV). This increasing in hardness resulted of addition of GO may be attributed to great mechanical properties of GO. As seen in table 2 and the SEM results (Figure 5) also confirm that the composites contain of 1 wt. % GO possess the more uniform and homogenous morphology rather than composites with 0.5 %wt GO. In addition, further addition of GO up to 2 wt. %, lead to form more porosities and agglomerates in the matrix being detrimental for mechanical properties. Overall, it seems that 1 wt. % GO is an optimal

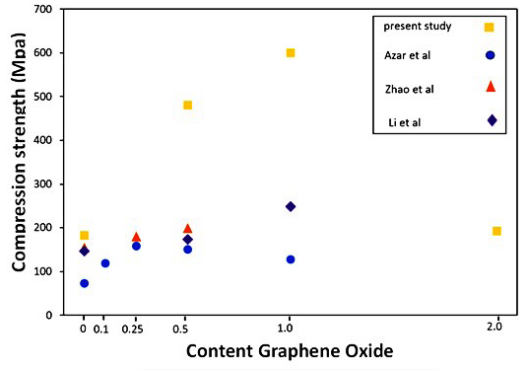

Fig. 8. Comparison of compression test results of this study with other similar researches.

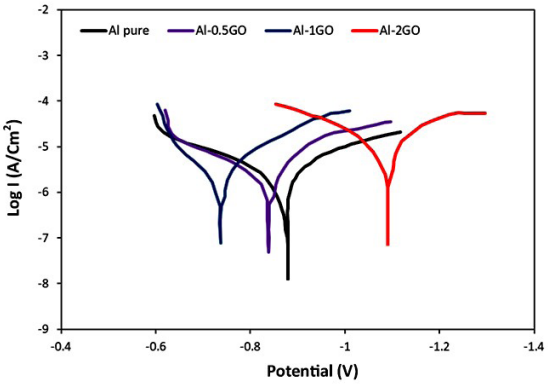

Fig. 9. The polarization curves of pure Al, Al-0.5GO, Al-1GO and Al-2GO in 3.5% NaCl.

amount that can be added to the composites in order to enhance the mechanical properties. The differences of hardness achieved from top and down of specimens' surfaces may be attributed to different grain size [37]. As indicated in Figure 6, the hardness of central areas is the highest and moving to the specimens' edges result in decrease in hardness.

The stress-strain curves of the composites are presented in Figure 7(a). Also, the values of yield and compression strength as function of GO content are illustrated in Figure 7(b). The highest compression strength (CS) and yield strength (YS) are belonged to Al-1GO where the compression and yield strength values are 600 and 295 MPa, respectively. These values are around 4 times higher than relative to pure Al (CS= 140 MPa, YS=70 MPa). The lower compression strength of Al-2GO (CS=170 MPa) in comparison with Al-0.5GO and Al-1GO is owing to formation of sever agglomerates throughout the Al matrix in composites.

As expected, by applying the RUE process in this work as a low temperature method (300 °C), we aimed to elaborate on the possible chemical reaction and resultant phases formation between Al and GO. So, in accordance to our obtained results, it can be infer that significant reaction did not occur in the system, particularly those leading to formation of a new phase such as Al_4C_3 along the Al and GO interfaces. The strengthening effect observed in the sample with 1 wt. % GO can be attributed to appropriate distribution of GO into the Al matrix and extraordinary strength of GO which may be led to noticeable transfer strength from Al to GO [38]. It should be noted that this load transferring depends on the strength of the interfacial bonding between Al and GO particles [39]. In additions, the other reason of mechanical properties enhancement of composites by adding the GO phase is the difference between thermal expansions of Al as matrix and GO as reinforcement phase (α_{GO}= -8×10^{-6} K^{-1}, α_{Al}= 23.6 ×10^{-6}K^{-1}) [40] which can be causing to formation of dislocation along the Al-GO interfaces depending

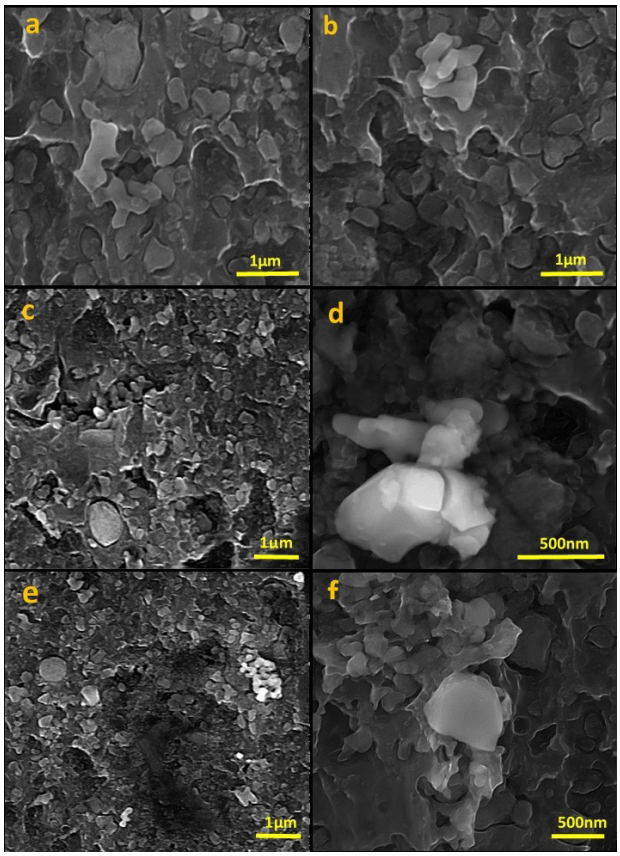

Fig. 10. SEM micrographs of (a) Pure Al (b) Al-0.5GO (c, d) Al-1GO (e, f) Al-2GO nanocomposites.

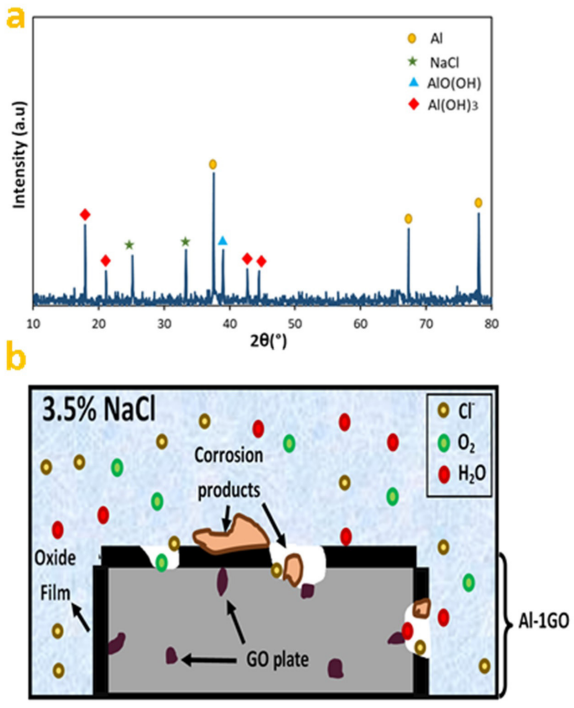

Fig. 11. (a) XRD pattern of corrosion products and (b) schematic describing corrosion mechanism for Al-GO nanocomposite.

Table 3.
Corrosion current densities and potentials obtained from polarization curve

Sample	Pure Al	Al-0.5GO	Al-1GO	Al-2GO
I_{corr} (μA/cm$_2$)	2.65	3.68	6.23	15.21
E_{corr} (V)	-0.860	-0.836	-0.750	-1.112

on surface area of GO [41]. As much as the GO particles are smaller, the dislocations densities are higher. In this situation, GO phases act as barriers against the dislocations movements throughout the Al matrix resulting in strengthening. The Figure 8 are presented the comparison of our compression tests results with other similar researches which on use from SPD methods [37,42,43]. These comparisons confirm the superiority of RUE rather than other similar methods in this area.

3.3. Electrochemical Behavior

Figure 9 shows the polarization curves of pure Al, Al-0.5GO, Al-1GO and Al-2GO in solution of 3.5% NaCl. The corresponding corrosion current density and the corrosion potential obtained from collision of anodic and cathodic slopes of polarization curves are tabulated in table 3.

By adding the 0.5 wt. % GO to the Al matrix, the corrosion current density increases (3.68 μA/cm^2), while the corrosion potential (-0.836 V) decreases rather to pure Al matrix (I_{corr}=2.65 μA/cm^2, E_{corr}= -0.860 V). Further addition of GO intensify the corrosion behaviors of composites as the corrosion density were 6.23 μA/cm^2 and 15.21 μA/cm^2 for 1 wt. % GO and 2 wt. % GO, respectively. This is why the corrosion potential demonstrates the falling trend as function of GO. The main reason for the increase in rate corrosion following the increase in amount of graphene oxide is the formation of galvanic corrosion between the aluminum and reinforcement. The FESEM images of pure Al, Al-0.5GO, Al-1GO and Al-2GO when were exposed to corrosion medium illustrated that the pure Al surface compared to other specimens are slightly corroded and further addition of GO up to 2wt. % cause to exacerbate the corrosion behaviors of composites (Figure 10). These findings are evidenced by polarization test results. In order to more investigate the corrosion by products of Al-1GO composites, the XRD test are prepared from corroded surface of sample. The results are shown in Figure 11(a). The schematic corrosion mechanism is also depicted in Figure 11(b). These are two common anodic and cathodic reactions for Al corrosions which are as follow:

$O_2+2H_2O+4e^-\rightarrow 4OH^-$ (Cathodic Reaction)

$Al\rightarrow Al^{3+}+3e^-$ (Anodic Reaction)

The dominant corrosion types in Al specimens are pitting corrosion. In composites contains of GO, the GO reinforcements act as cathodes and formed void throughout the composites could degrade the continuity of Al_2O_3 passive film forming on the Al surface. These occurrences cause to dissolve the Al matrix and form the Al $(OH)_3$ and AlO (OH) phases. It is obvious that the GO phase due to formation of voids and porosities along the Al as matrix and GO as reinforcement interfaces cause to worse the corrosion resistance of composites. The findings are agreed with similar results reported by Rashed et al. [38] and Askarnia et al. [23].

4. Conclusions

In the current study, the fabrication of Al with different contents of GO composites via RUE method was performed. From the results of this study, the following conclusions can be pointed out:

- The great dispersion of GO throughout the Al matrix was achieved for Al-1GO composites and further additions of GO in Al matrix due to higher surface area of GO and sever tendencies to the agglomerations decreased the uniformity and homogeneity of GO distributions in Al matrix.
- No adverse reactions occurred between Al and GO during the RUE process which approved by XRD and Raman results.
- The highest hardness among the all composites belongs to the Al-1GO with 137 HV as well as yield and compression strengths. Further addition of GO content (up to 2 wt. %) led to 248 % decrease in mechanical properties (CS=170 MPa) rather than Al-1GO.
- The presence of carboxyl (C=O bond) in FTIR of Al-1GO after RUE operation indicates that GO is not converted to RGO.
- Composite with 2% GO has higher I_{corr} (15.21 μA/cm^2) than the bare Al (2.65 μA/cm^2) due to the effect of graphene oxide in the form of galvanic corrosion.
- Corrosion products were Al $(OH)_3$ and AlO (OH) phases for Al-1GO sample.

Acknowledgments

The authors would like to acknowledge Semnan University for the financial support towards this research.

Conflict of interest

The authors declare that there is no conflict of interest.

REFERENCES

[1] S.T. Mavhungu, E.T. Akinlabi, M.A. Onitiri, F.M. Varachia, Aluminum Matrix Composites for Industrial Use: Advances and Trends, Procedia Manufacturing 7 (2017) 178–182.
[2] M. Rezayat, A. Akbarzadeh, A. Owhadi, Production of high strength Al-Al$_2$O$_3$ composite by accumulative roll bonding, Composites Part A: Applied Science and Manufacturing 43(2) (2012) 261–267.
[3] S.P. Dwivedi, Microstructure and mechanical behaviour of Al/B$_4$C metal matrix composite, Materials Today: Proceedings 25 Part4 (2020) 751–754.
[4] S.M.A.K. Mohammed, D.L. Chen, Carbon Nanotube-Reinforced Aluminum Matrix Composites, Advanced Engineering Materials 22(4) (2020) 1901176.
[5] S.R. Fardi, H. khorsand, R. Askarnia, R. Pardehkhorram, E. Adabifiroozjaei, Improvement of biomedical functionality of titanium by ultrasound-assisted electrophoretic deposition of hydroxyapatite-graphene oxide nanocomposites, Ceramics International 46(11, Part A) (2020) 18297–18307.
[6] R. Askarnia, S.R. Fardi, M. Sobhani, H. Staji, Ternary hydroxyapatite/chitosan/graphene oxide composite coating on AZ91D magnesium alloy by electrophoretic deposition, Ceramics International 47(19) (2021) 27071–27081.
[7] R. Askarnia, B. Ghasemi, S.R. Fardi, E. Adabifiroozjaei, Improvement of tribological, mechanical and chemical properties of Mg alloy (AZ91D) by electrophoretic deposition of alumina/GO coating, Surface and Coatings Technology 403 (2020) 126410.
[8] Y. Estrin, A. Vinogradov, Extreme grain refinement by severe plastic deformation: A wealth of challenging science, Acta Materialia 61(3) (2013) 782–817.
[9] N.Q. Chinh, P. Jenei, J. Gubicza, E. V. Bobruk, R.Z. Valiev, T.G. Langdon, Influence of Zn content on the microstructure and mechanical performance of ultrafine-grained Al–Zn alloys processed by high-pressure torsion, Materials Letters 186 (2017) 334–337.
[10] M. Alizadeh, M.H. Paydar, F. Sharifian Jazi, Structural evaluation and mechanical properties of nanostructured Al/B$_4$C composite fabricated by ARB process, Composites Part B: Engineering 44(1) (2013) 339–343.
[11] B.P. Dileep, H.R. Vitala, V. Ravi Kumar, M.M. Suraj, Effect of ECAP on Mechanical and Micro-Structural Properties of Al7075-Ni Alloy, Materials Today Proceedings 5(11, Part3) (2018) 25382–25388.
[12] P. Veena, D.M. Yadav, C.N. Kumar, A Critical Review on Severe Plastic Deformation, International Journal of Scientific Research in Science, Engineering and Technology 3(2) (2017) 336–343.
[13] J.K. Tiwari, A. Mandal, N. Sathish, V.A.N. Ch, A.K. Srivastava, Graphene platelets reinforced aluminum matrix composite with enhanced strength by hot

accumulative roll bonding, arXiv e-prints (2018) arXiv-1807.
[14] B. Schuh, F. Mendez-Martin, B. Völker, E.P. George, H. Clemens, R. Pippan, A. Hohenwarter, Mechanical properties, microstructure and thermal stability of a nanocrystalline CoCrFeMnNi high-entropy alloy after severe plastic deformation, Acta Materialia 96 (2015) 258–268.
[15] S.F. Bartolucci, J. Paras, M.A. Rafiee, J. Rafiee, S. Lee, D. Kapoor, N. Koratkar, Graphene-aluminum nanocomposites, Materials Science and Engineering: A 528(27) (2011) 7933–7937.
[16] H. Zhang, C. Xu, W. Xiao, K. Ameyama, C. Ma, Enhanced mechanical properties of Al5083 alloy with graphene nanoplates prepared by ball milling and hot extrusion, Materials Science and Engineering: A 658 (2016) 8–15.
[17] T. Faraji Shovay, S. Ghaemi Khiavi, E. Emadoddin, H.-R. M. Semnani, Repetitive Upsetting Extrusion Process of Al5452 Alloy: Finite Element Analysis and Experimental Investigation, Iranian Journal of Materials Forming 8(1) (2021) 65–74.
[18] G. Zhang, Z. Zhang, Y. Meng, Z. Yan, X. Che, X. Li, Effects of repetitive upsetting extrusion on the microstructure and texture of GWZK124 alloy under different starting temperatures, Materials 12(15) (2019) 2437.
[19] A. Wiśniewska, S. Hernik, A. Liber-Kneć, H. Egner, Effective properties of composite material based on total strain energy equivalence, Composites Part B: Engineering 166 (2019) 213–220.
[20] R. Atif, F. Inam, Reasons and remedies for the agglomeration of multilayered graphene and carbon nanotubes in polymers, Beilstein Journal of Nanotechnology 7 (2016) 1174–1196.
[21] M.A. Ashraf, W. Peng, Y. Zare, K.Y. Rhee, Effects of Size and Aggregation/Agglomeration of Nanoparticles on the Interfacial/Interphase Properties and Tensile Strength of Polymer Nanocomposites, Nanoscale Research Letters 13 (2018) 214.
[22] B. Binesh, M. Aghaie-Khafri, Microstructure and texture characterization of 7075 Al alloy during the SIMA process, Materials Characterization 106 (2015) 390–403.
[23] R. Askarnia, B. Ghasemi, S.R. Fardi, H.R. Lashgari, E. Adabifiroozjaei, Fabrication of high strength aluminum-graphene oxide (GO) composites using microwave sintering, Advanced Composite Materials 30(3) (2021) 271–285.
[24] G. Li, B. Xiong, Effects of graphene content on microstructures and tensile property of graphene-nanosheets / aluminum composites, Journal of Alloys and Compounds 697 (2017) 31–36.
[25] H. Kwon, M. Estili, K. Takagi, T. Miyazaki, A. Kawasaki, Combination of hot extrusion and spark plasma sintering for producing carbon nanotube reinforced aluminum matrix composites, Carbon 47(3) (2009) 570–577.
[26 E.I. Bîru, H. Iov, Graphene Nanocomposites Studied by Raman Spectroscopy, IntechOpen, Croatia, 2018.
[27] Y. Jiang, S. Deng, S. Hong, J. Zhao, S. Huang, C.C. Wu, J.L. Gottfried, K.I. Nomura, Y. Li, S. Tiwari, R.K. Kalia, P. Vashishta, A. Nakano, X. Zheng, Energetic Performance of Optically Activated Aluminum/Graphene Oxide Composites, ACS Nano 12(11) (2018) 11366–11375.
[28] G. Fan, Y. Jiang, Z. Tan, Q. Guo, D. bang Xiong, Y. Su, R. Lin, L. Hu, Z. Li, D. Zhang, Enhanced interfacial bonding and mechanical properties in CNT/Al composites fabricated by flake powder metallurgy, Carbon 130 (2018) 333–339.
[29] B. Chen, K. Kondoh, H. Imai, J. Umeda, M. Takahashi, Simultaneously enhancing strength and ductility of carbon nanotube/aluminum composites by improving bonding conditions, Scripta Materialia 113 (2016) 158–162.
[30] S. Pei, H.M. Cheng, The reduction of graphene oxide, Carbon 50(9) (2012) 3210–3228.
[31] S.R.B. Nazri, W.W. Liu, C.S. Khe, N.M.S. Hidayah, Y.P. Teoh, C.H. Voon, H.C. Lee, P.Y.P. Adelyn, Synthesis, characterization and study of graphene oxide, AIP Conference Proceedings 2045(1) (2018) 020033.
[32] T. Rattana, S. Chaiyakun, N. Witit-Anun, N. Nuntawong, P. Chindaudom, S. Oaew, C. Kedkeaw, P. Limsuwan, Preparation and characterization of graphene oxide nanosheets, Procedia Engineering 32 (2012) 759–764.
[33] M. Acik, G. Lee, C. Mattevi, A. Pirkle, R.M. Wallace, M. Chhowalla, K. Cho, Y. Chabal, The role of oxygen during thermal reduction of graphene oxide studied by infrared absorption spectroscopy, The Journal of Physical Chemistry C 115(40) (2011) 19761–19781.
[34] D.C. Marcano, D. V. Kosynkin, J.M. Berlin, A. Sinitskii, Z. Sun, A. Slesarev, L.B. Alemany, W. Lu, J.M. Tour, Improved synthesis of graphene oxide, ACS Nano 4(8) (2010) 4806–4814.
[35] R. Shu, X. Jiang, H. Sun, Z. Shao, T. Song, Z. Luo, Recent researches of the bio-inspired nano-carbon reinforced metal matrix composites, Composites Part A: Applied Science and Manufacturing 131 (2020) 105816.
[36] M. Rashad, F. Pan, A. Tang, M. Asif, Effect of Graphene Nanoplatelets addition on mechanical properties of pure aluminum using a semi-powder method, Progress in Natural Science: Materials International 24(2) (2014) 101–108.
[37] M.H. Azar, B. Sadri, A. Nemati, S. Angizi, M.H. Shaeri, P. Minárik, J. Veselý, F. Djavanroodi, Investigating the microstructure and mechanical properties of aluminum-matrix reinforced- graphene nanosheet composites fabricated by mechanical milling and equal-channel angular pressing, Nanomaterials 9(8) (2019) 1070.
[38] M. Rashad, F. Pan, Z. Yu, M. Asif, H. Lin, R. Pan, Investigation on microstructural, mechanical and electrochemical properties of aluminum composites reinforced with graphene nanoplatelets, Progress in Natural Science: Materials International 25(5) (2015) 460–470.
[39] W. ming Tian, S. mei Li, B. Wang, X. Chen, J. hua Liu, M. Yu, Graphene-reinforced aluminum matrix composites prepared by spark plasma sintering, International Journal of Minerals, Metallurgy, and Materials 23 (2016) 723–729.
[40] D. Yoon, Y.W. Son, H. Cheong, Negative thermal expansion coefficient of graphene measured by raman spectroscopy, Nano Letters 11(8) (2011) 3227–3231.
[41] W. Zhou, Y. Fan, X. Feng, K. Kikuchi, N. Nomura, A. Kawasaki, Creation of individual few-layer graphene incorporated in an aluminum matrix, Composites Part A: Applied Science and Manufacturing 112 (2018) 168–177.
[42] L. Zhao, H. Lu, Z. Gao, Microstructure and Mechanical Properties of Al/Graphene Composite Produced by High-Pressure Torsion, Advanced Engineering Materials 17(7) (2015) 976–981.
[43] J.L. Li, Y.C. Xiong, X.D. Wang, S.J. Yan, C. Yang, W.W. He, J.Z. Chen, S.Q. Wang, X.Y. Zhang, S.L. Dai, Microstructure and tensile properties of bulk nanostructured aluminum/graphene composites prepared via cryomilling, Materials Science and Engineering: A 626 (2015) 400–405.